AFRL-IF-RS-TR-2004-93
Final Technical Report
April 2004

OPTOFLOW: DESIGN TOOLS FOR INTEGRATING OPTICAL DETECTION IN MICRO-TOTAL ANALYSIS SYSTEMS

Coventor, Inc.

Sponsored by
Defense Advanced Research Projects Agency
DARPA Order No. K900

APPROVED FOR PUBLIC RELEASE; DISTRIBUTION UNLIMITED.

The views and conclusions contained in this document are those of the authors and should not be interpreted as necessarily representing the official policies, either expressed or implied, of the Defense Advanced Research Projects Agency or the U.S. Government.

AIR FORCE RESEARCH LABORATORY
INFORMATION DIRECTORATE
ROME RESEARCH SITE
ROME, NEW YORK

STINFO FINAL REPORT

This report has been reviewed by the Air Force Research Laboratory, Information Directorate, Public Affairs Office (IFOIPA) and is releasable to the National Technical Information Service (NTIS). At NTIS it will be releasable to the general public, including foreign nations.

AFRL-IF-RS-TR-2004-93 has been reviewed and is approved for publication.

APPROVED: /s/
PETER J. ROCCI
Project Engineer

FOR THE DIRECTOR: /s/
JAMES A. COLLINS, Acting Chief
Information Technology Division
Information Directorate

REPORT DOCUMENTATION PAGE

Form Approved
OMB No. 074-0188

Public reporting burden for this collection of information is estimated to average 1 hour per response, including the time for reviewing instructions, searching existing data sources, gathering and maintaining the data needed, and completing and reviewing this collection of information. Send comments regarding this burden estimate or any other aspect of this collection of information, including suggestions for reducing this burden to Washington Headquarters Services, Directorate for Information Operations and Reports, 1215 Jefferson Davis Highway, Suite 1204, Arlington, VA 22202-4302, and to the Office of Management and Budget, Paperwork Reduction Project (0704-0188), Washington, DC 20503

1. AGENCY USE ONLY (Leave blank)	2. REPORT DATE	3. REPORT TYPE AND DATES COVERED
	APRIL 2004	**FINAL** **Sep 01 – Sep 03**

4. TITLE AND SUBTITLE
OPTOFLOW: DESIGN TOOLS FOR INTEGRATING OPTICAL DETECTION IN MICRO-TOTAL ANALYSIS SYSTEMS

5. FUNDING NUMBERS
G - F30602-01-2-0547
PE - 61101E
PR - E117
TA - 00
WU - 72

6. AUTHOR(S)

Tom Korsmeyer

7. PERFORMING ORGANIZATION NAME(S) AND ADDRESS(ES)

Coventor, Inc.
215 First Street
Cambridge MA 02142

8. PERFORMING ORGANIZATION REPORT NUMBER

N/A

9. SPONSORING / MONITORING AGENCY NAME(S) AND ADDRESS(ES)

Defense Advanced Research Projects Agency
3701 North Fairfax Drive
Arlington VA 22203-1714

AFRL/IFTB
525 Brooks Road
Rome NY 13441-4505

10. SPONSORING / MONITORING AGENCY REPORT NUMBER

AFRL-IF-RS-TR-2004-93

11. SUPPLEMENTARY NOTES

AFRL Project Engineer: Peter J. Rocci/IFTB/(315) 330-4654 Peter.Rocci@rl.af.mil

12a. DISTRIBUTION / AVAILABILITY STATEMENT

APPROVED FOR PUBLIC RELEASE; DISTRIBUTION UNLIMITED.

12b. DISTRIBUTION CODE

13. ABSTRACT ***(Maximum 200 Words)***

The finest systems for chemical and microchemical analysis today use optical systems for detection and identification of chemical samples. This is because these systems offer both the highest sensitivity and can make use of the most powerful array of labeling and tagging technologies to give specificity to any measurement. The major drawback of such optical subsystems for DoD applications in chemical and biological warfare detection (CBD) is their large size, high cost, and relative fragility. Given the recent progress in integrated microfluidics, in optical MEMS, and in passive micro-optics, the time is right to drive high quality optical detection systems for microchemistry to compact micro-fabricated implementations.

14. SUBJECT TERMS
Simulation, CAD Tools, Microchemical Systems, Optical Microsystems

15. NUMBER OF PAGES 17

16. PRICE CODE

17. SECURITY CLASSIFICATION OF REPORT	18. SECURITY CLASSIFICATION OF THIS PAGE	19. SECURITY CLASSIFICATION OF ABSTRACT	20. LIMITATION OF ABSTRACT
UNCLASSIFIED	UNCLASSIFIED	UNCLASSIFIED	UL

Table of Contents

List of Figures

1.0 Introduction

The key to enabling design of integrated optical subsystems in BioMEMS or micro- Total Analysis Systems (μ-TAS) systems is to help designers cope with co-design problems. These are the problems that arise at the interfaces between microsystem domains. In microfluidic systems most devices are often at the intersection of all three domains. As a result, the design process would be greatly facilitated by a tool that allows such co-design problems. The interface areas in typical microfluidic systems lie between the optical, MEMS and fluidic domains. Here, we propose to build tools for the effective design of systems at the intersection of the optical and fluidic domains. In the design of detectors for biological and chemical microsystems, several design issues arise. In general, sample concentrations that need to be detected are very small - often only a few molecules. This requires a very efficient mechanism of optical collection. Detection limits for biological fluorescence are often set by the presence of other light sources derived from the optical excitation beam. The DC component of these sources can generally be subtracted, but the photon-shot-noise from them cannot be and often determines the detection threshold. In addition, the biological fluorescence signal must compete with shot-noise on stary-light from the excitation source. This will include scatter in both the microfluidics and the micro-optics. The ability to design optical detection systems that account for these issues is critical, but is currently hampered by the unavailability of design tools that explore this space. This effort aims at developing a methodology and associated tools to enable this design. The tools incorporate state-of-the-art detailed modeling techniques for both the optical component modeling as well as the fluidic modeling as well as reduced-order model extraction and simulation for the entire system. The system modeling allows the coupling of the opto-fluidic component models with MEMS and IC domain models that are in Coventor's design suite or are in development at Coventor. Past DARPA funded work in fluidic system modeling (Composite CAD program) and past and future related work in the telecommunications, optics and opto-electronics domains were integrated and leveraged.

2.0 Detailed Modeling

OptoFlow task has two specific sub-tasks. First is the development of a detailed model describing the fluidic detection region that captures the state of the sample in the detection region and the illumination of the sample by the incident light. The second sub-task is the development of detailed modeling capabilities for the optical components in the integrated system. The two sub-tasks will then be coupled to enable the modeling of the optical detection problem.

The fluidic detection modeling sub-task is an extension of the tools developed under previous DARPA programs (NetFlow and FlumeCAD) to encompass the additional relevant physics required to model the detection region. Figure 1 shows a typical simulation example. The fluid is switched electrokinetically from the intersection between two channels into a separation column. The individual species have different electrokinetic and diffusion properties that cause them to separate as they travel down the separation column. The detection region is defined by a specific volume in the separation column. Light emitted by the species traveling through the detection region is collected optically to record the band width and separation of the sample. The optical

component modeling sub-task is eventually expected to use a scalar and rigorous electromagnetic simulation of these optical components. This sub-task will employ the Finite Difference Time Domain (FDTD) method in the solution of the Maxwell equations to address the light scattering problem. Application of the FDTD method to the fluid detection region presents some fundamental challenges due to the size of the fluid volume compared to the wavelength of light. Our initial focus in this sub-task is to develop techniques to reduce the computational intensity of the Maxwell problem to make this analysis more tractable.

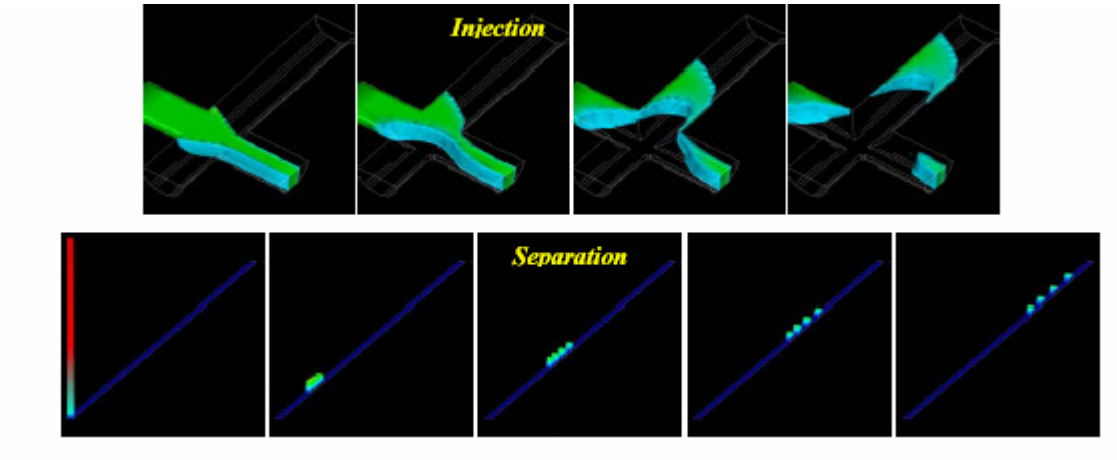

Figure 1: Typical Separation Simulation through Coventorware.

Our approach in this task is to develop tools of increasing complexity for the detailed modeling of the detection region. The simplest model assumes an ideal detector – that is, all light emitted by the sample band is collected at the detector. The signal collected using this model is shown in Figure 2, as a crossover plot defining the highest resolvable fragment that is detectable. The crossover plot is a typical measure of the resolution of the separation column. As the figure shows the resolution of the ideal detector is very near the analytically predicted resolution. The difference between the two is the result of the initial band shape – the analytical detector assumes a rectangular band, whereas the simulation distributes it over several computational cells. The model complexity is increased by treating the incident light as a finite-width gaussian beam. The light emitted by the sample band, traveling through the detection region, is modulated by the incident Gaussian beam shape. The net effect is a reduction in the signal in comparison to the ideal detector signal. This is shown in Figure 3. Here the crossover plots are shown for several different detector widths. The fall-off in the resolution due to the Gaussian beam is evident in the figure. As expected, a wider detection region results in lower resolution.

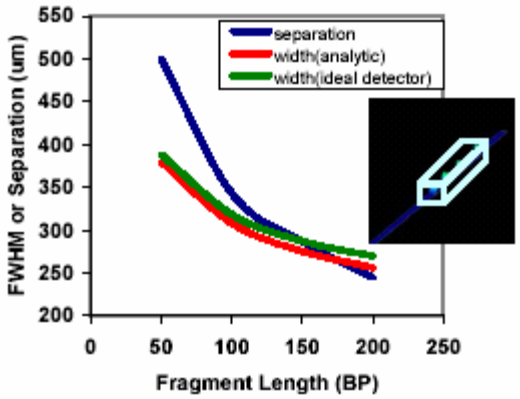

Figure 2: Crossover Plot showing resolution of Separation Column using ideal detector

The next step is to develop a model for the light absorption by a finite sample concentration in the detection region. Furthermore, the absorbed light is emitted isotropically and, in addition, only a portion of the light is assumed captured by the detector, based on its position and size and on additional collection optics. The varying species in the detection region can also be discriminated by a molar extinction coefficient that defines the fraction of incident light absorbed by the sample molecules.

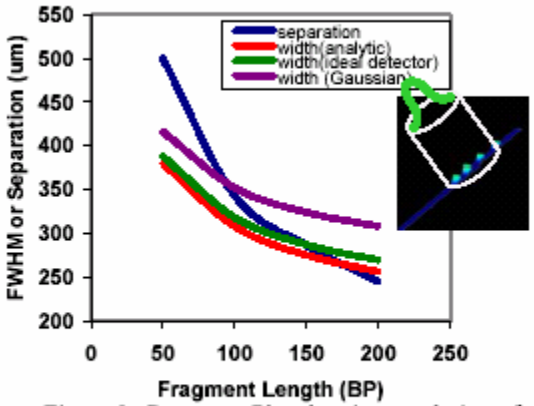

Figure 3: Crossover Plot showing resolution of Separation Column using Gaussian Detector compared to ideal.

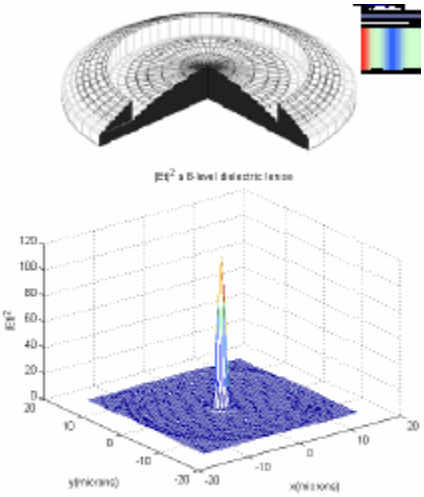
Figure 4: FDTD Design Analysis of Dielectric Lens

3.0 Library of Parameterized Models

This task is targeted at developing a library of parameterized models for optical detection systems and the tools to co-design the optical models with models for the μTAS system. In this task, we leverage the existing optical modeling work that is underway at Coventor. This has been targeted directly at the telecom and optoelectronic spaces but must now be extended to include the fluidic space as well. The fluidic space offers different challenges – the components are different as well as the application space.

The basic components required in modeling the detection problem are the light source and focusing optics to focus the incident beam on the detection region and collection optics and a detector for collecting the emitted light. The initial focus of this work is targeted at developing models for these components, in order to try and develop a model for a microscope that can be used in sample detection. These models are designed to work in conjunction with the fluidic models in the Fluids Library (originally developed under the FlumeCAD contract) as well as the optical models in Coventor's optical library.

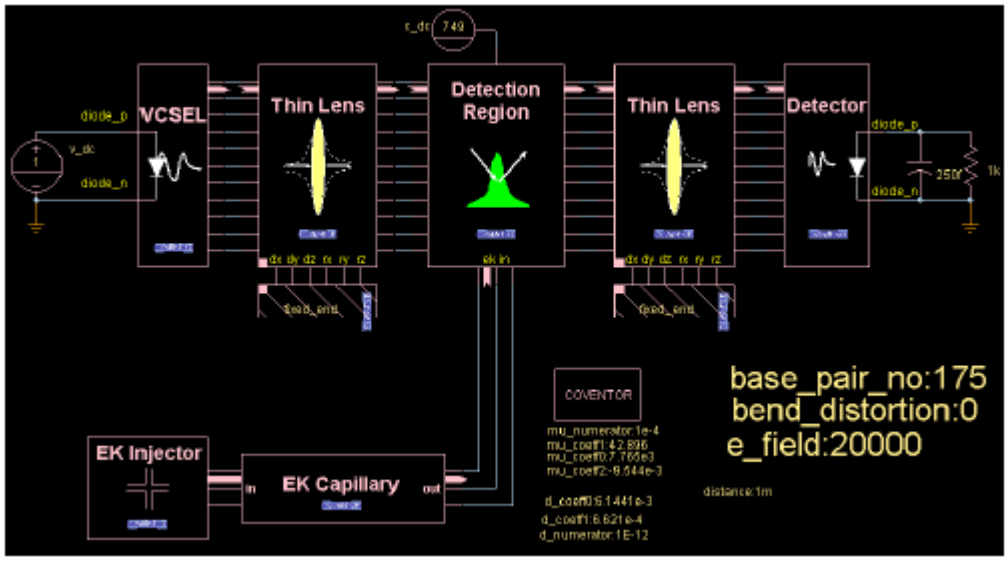

Figure 5: Basic Fluorescence Detection System Model. The various libraries in CoventorWare can be linked together to solve the coupled sample transport and detection problem.

We have developed models for these basic components and integrated them with models for the gaussian optics and the fluidic components to build an integrated model for the chemical transport and detection problem. One example of a schematic is shown in Figure 5. The individual libraries that the models originate from are:

FluidsLibrary Models: These are the sample transport models including electrokinetic injection and the separation column. This library is part of CoventorWare and its development was initiated through the FlumeCAD program.

Mems-Optics Models: These are the gaussian optics models that are part of the CoventorWare Architect suite. The light source (VCSEL) and focusing optics are part of this library. Note that the Gaussian light source assumption is valid in these detection problems.

FluidsLib Extension: The "fluidic" portion of the detection region is represented by the Detection Region model, developed under this program. The detection region captures the sample location and concentration and models the absorption and emission of the light by the sample. The initial version of this model used here is purely one-dimensional – that is, the sample concentration is assumed to be uniform along the width and depth of the channel.

OptoDetLib Models: The OptoDetLib models represent the collection optics and the detector where the emitted light from the sample is collected and transduced to a measurable signal. In general, this may include collection optics such as DOE's or lenses, filters, stops, detectors, stray light absorbers and so on. The initial set of models under development are the basic DOE's/lens models and a detector model. Several typical microscope models and detection schemes can be modeled purely with DOE's and detectors as the collection optics. Enhancements and extensions to other models will follow in later versions of the library.

The operation of the models is shown in Figures 6-7. Two discrete samples flowing through the detection region absorb the incident light and emit it to the detector where it is collected. The absorption is based on a simple Beer-Lambert law approximation. This approximation is actually quite valid in biological detection because, in most cases, there is considerably more incident light than required to excite the sample molecules. The collected light on the detector is shown in Figure 6 for the two bands traveling down the channel. The width of the bands is determined by their electrokinetic mobility and diffusivity – which in turn is typically a function of the charge-to-mass ratio – larger fragments move slower and diffuse less than smaller fragments – as a result they tend to render on the detector with lower amplitude and larger band width.

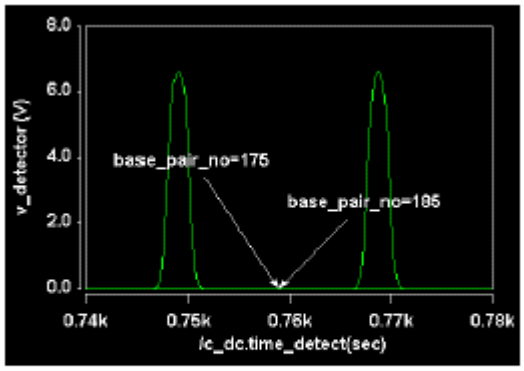

Figure 6: SeparationAnalysis using Detection Model from Figure 5.

The system model has the advantage of allowing rapid analyses of a wide range of design variations in the system. Examples of these are shown in Figures 7-9. The dependence of the signal on the distance of the collection optics from the detection region is shown in Figure 7 – the signal strength increases as the detection region comes into focus and decays as the distance increases further and the region goes out of focus. A similar effect is seen for increasing the distance of the light source from the detection region as shown in Figure 8. Figure 9 shows the variation in the signal due to incorrect alignment of the detector with the light from the detection region. The ideal alignment of the detector is at 45° to the channel (in this case) so as to maintain orthogonality between the detector and the collection DOE lens. The signal falloff as the detector is rotated into the ideal position and away from it can be seen in the figure. An important point to note here is that, in this particular example, the signal strength is not very sensitive to the detector alignment at small

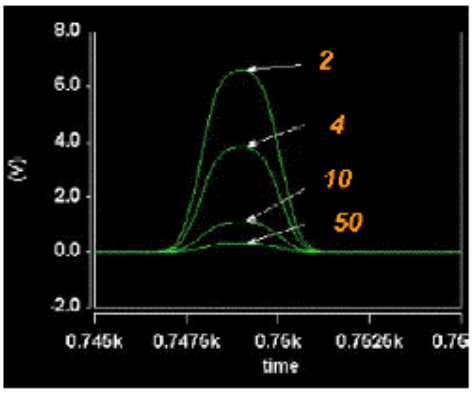

Figure 7: Signal dependence on distance of detector from detection region.

angles. This is a useful result in the design of optical systems, since misalignment is often one of the more common causes of signal loss.

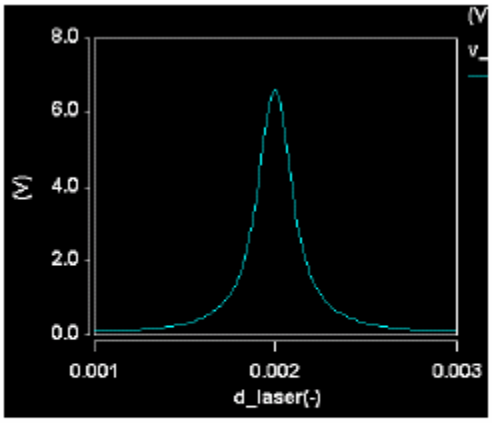

Figure 8: Signal dependence on distance of light source from detection region.

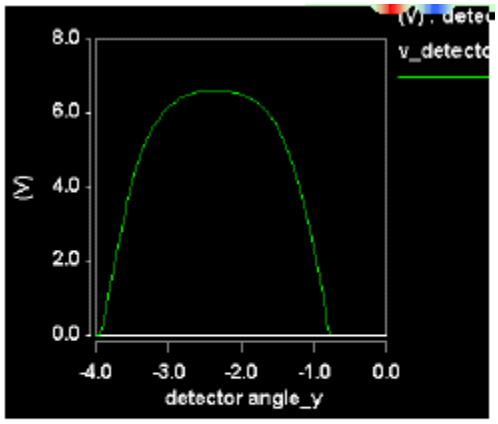

Figure 9: Signal dependence on alignment of detector

4.0 Experimental Validation

The experimental validation task has two distinct purposes – first, the generation of validation data to support the detailed simulation and model building efforts, and, second, to demonstrate the integration of the optical and fluidic subsystems. These subsystems form two distinct subtasks in the experimental validation task in this program. The fluidic subsystem task is aimed at building typical biological devices that can be matched to optical components, either discrete, or integrated on an adjoining layer. The optical subsystem task is aimed at building these microfabricated optical components.

Due to DARPA funding limitations and subsequent early termination of this effort, all validation subtasks could not be completed. The generation and validation of data to support the detailed simulation and model building efforts was not accomplished. The fluidic subsystem task was not completed either. The information presented here is related to the optical subsystem task.

Experimental investigations at the University of Delaware have been focused around developing the necessary technology to build microfabricated lenses. After reviewing potential material options, we decided to fabricate the initial devices in AZ5214 photoresist on microscope slide substrates. Some of the issues related to using AZ5214 photoresist included:

- Index of refraction data for the wavelengths of interest
- Spincoating speeds for the correct thickness
- Absorption and fluorescence of the photoresist at operating wavelengths.

Index of Refraction Data

The index of refraction data for AZ5214 was found on the Clariant website for AZ Electronic Materials, http://www.azresist.com. Cauchy Constants are provided for bleached and unbleached resist.

	Bleached	Unbleached
Thickness (nm)	1390.3	1414.7
A	1.5908	1.6035
B (μm^2)	0.011525	0.0055741
C (μm^2)	6.70×10^{-7}	2.34×10^{-3}

Using the Cauchy formula, $n=A+B/\lambda^2+C/\lambda^4$, the following data was generated.

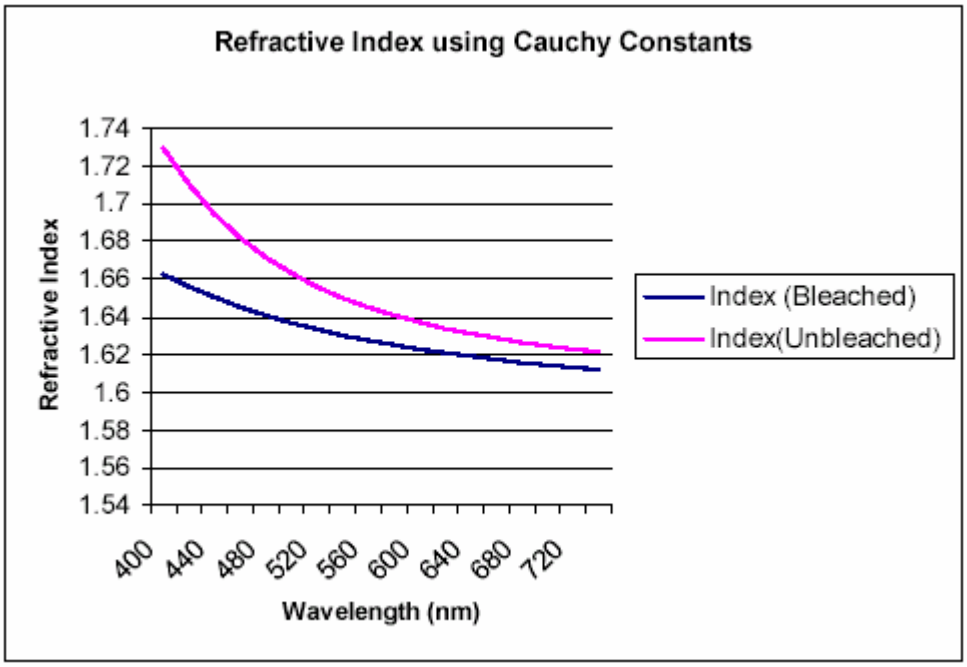

Figure 10: Index of Refraction vs. Wavelength

If bleached resist is fully exposed and developed, then for 455 nm, the index of refraction is approximately 1.65. For a 2π phase shift, the height or thickness of resist can be determined by the formula, $h=\lambda/(n-1)$. Thus, for 455 nm, the thickness of the diffractive lens should be 700 nm.

Spin-Coating Data

Softbake film thicknesses for 3000 to 7000 rpm are reported in the AZ 5200 Positive Photoresist literature. At 7000 rpm, the film thickness is approximately 1.0 µm. From previous work, we know that spinning at 10,000 rpm for 40 seconds results in a 0.5 µm thickness. See Figure 2. Since we are interested in film thicknesses of 0.7µm, then we estimate that spin speeds should be around 8000 rpm.

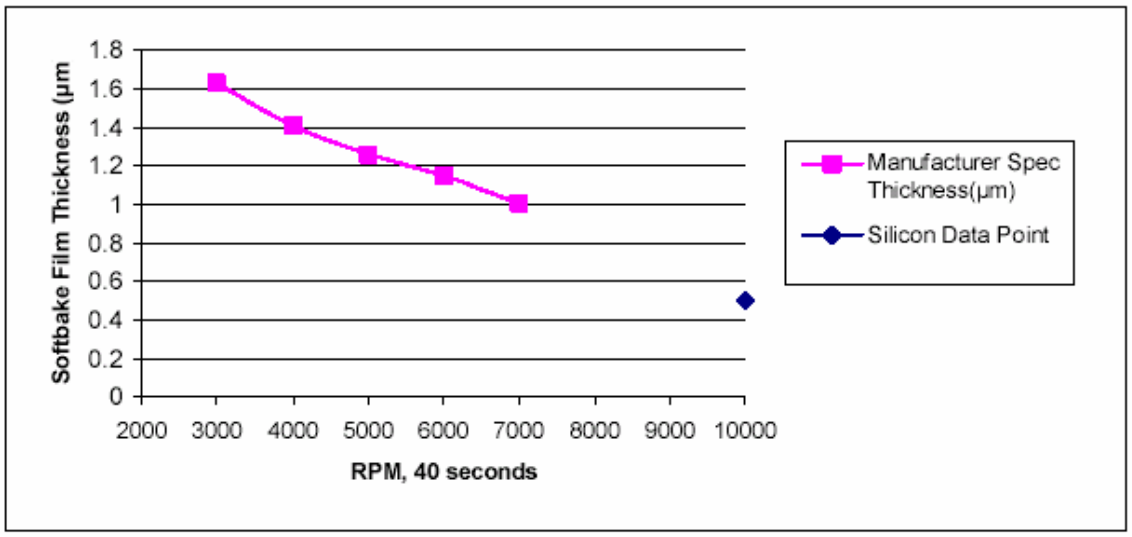

Figure 11: Film Thickness vs. RPM

A diffractive lens that was fabricated with an 8000 rpm spin speed is shown in Figure 12. Using a WYKO RST surface profiler, the lens height was measured to be 633nm. Thus spin speeds slightly less 8000 rpm will be appropriate for 455 nm operating wavelengths.

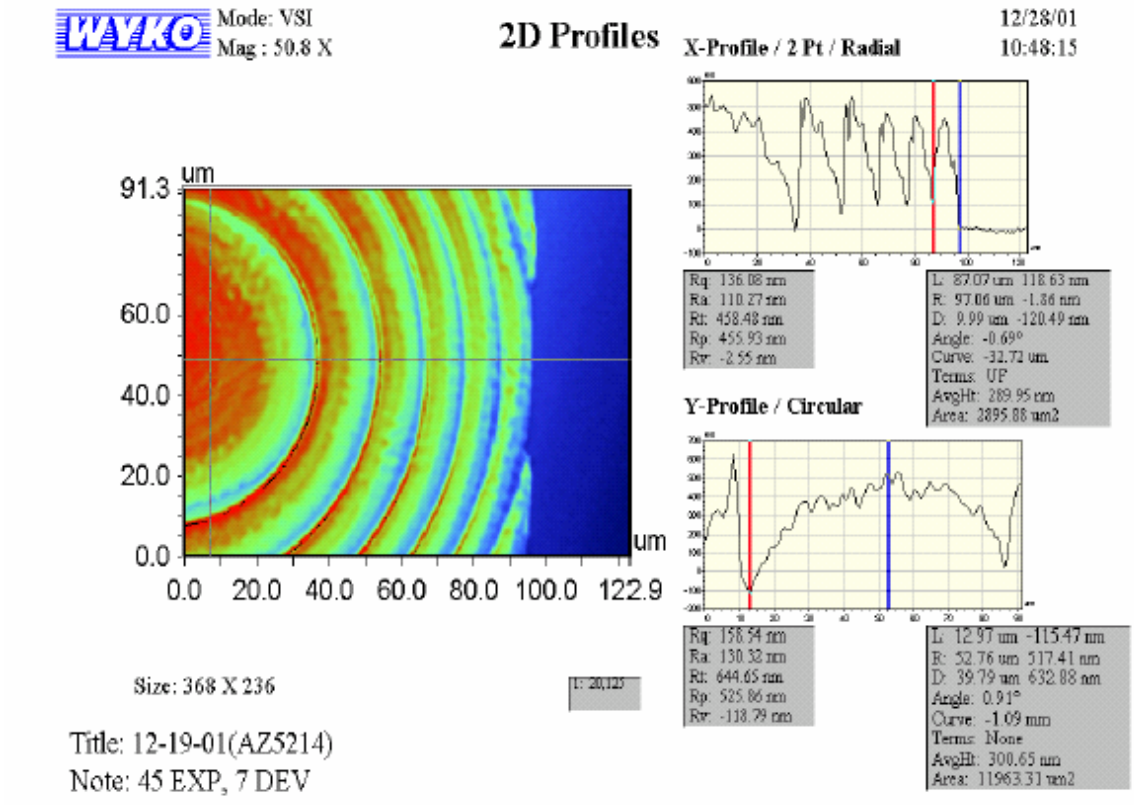

Figure 12: Diffractive Surface in AZ5314 Photoresist, 8000 rpm spin speed

Transmission Measurements from 400nm to 700nm

Data from the manufacturer reports that for wavelengths above 400 nm, the transmission for a 1 μm thick layer of exposed resist should be greater than 95%. For unexposed resist, the transmission is 50% at 400 nm and increases almost linearly to 95% at 450 nm. Thus, if the photoresist is fully exposed after fabrication, it is likely that transmission will be high enough for good performance.

To verify this data, a simple experiment was devised to measure transmission losses through photoresist films on microscope slides. We considered the following cases for this study.

- Blank microscope slide, no resist.
- Unexposed resist on microscope slide.
- Exposed resist on microscope slide.
- Unexposed resist followed by AZ327MIF development
- Unexposed resist followed by AZ327MIF development then exposed.

All samples were softbaked at 90 degrees C for 30 seconds after application of photoresist material.

Using an Ando AQ-4303B White Light Source that was coupled to a fiber, light was directed through a test slide and refocused by a microscope objective into another fiber. That fiber was inserted into an Agilent 86140B Optical Spectrum Analyzer that was configured to measure the transmission from 400 nm to 700 nm. The test arrangement is shown in Figures 13 and 14.

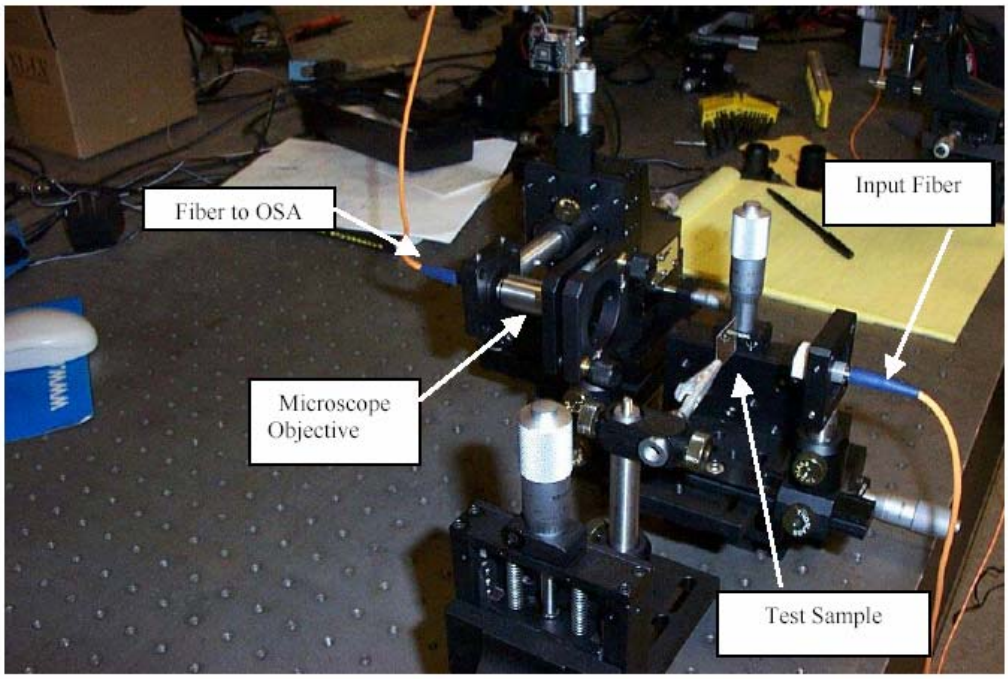

Figure 13: Transmission Measurement Set Up

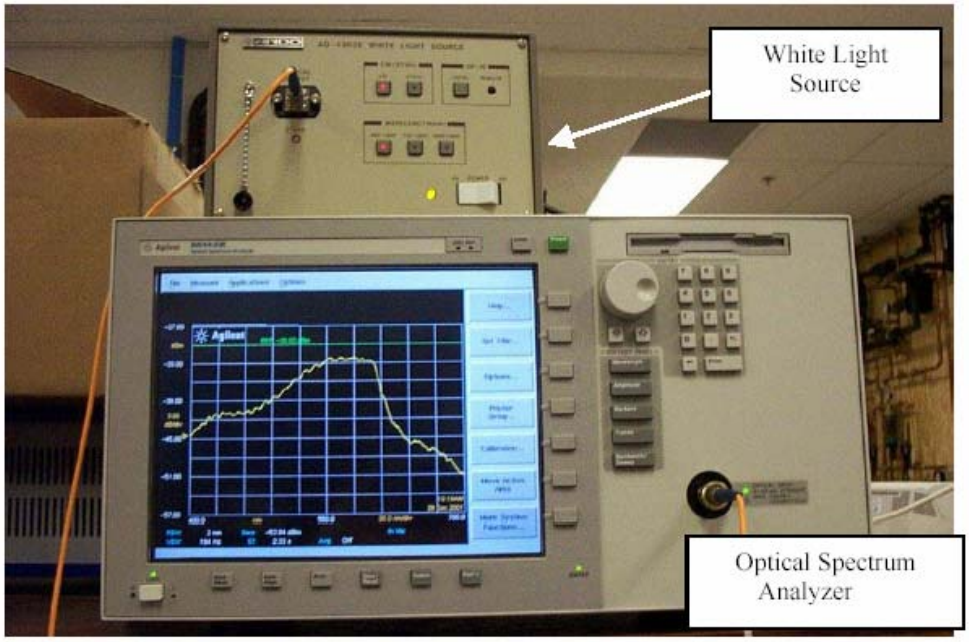

Figure 14: White Light Source and Optical Spectrum Analyzer

Each of the 5 samples listed above was placed in the set up. The position of the microscope objective was then adjusted to maximize the overall transmission. In addition, the transmission was measured with no slide to establish a baseline. The results of these measurements are shown in Figure 15.

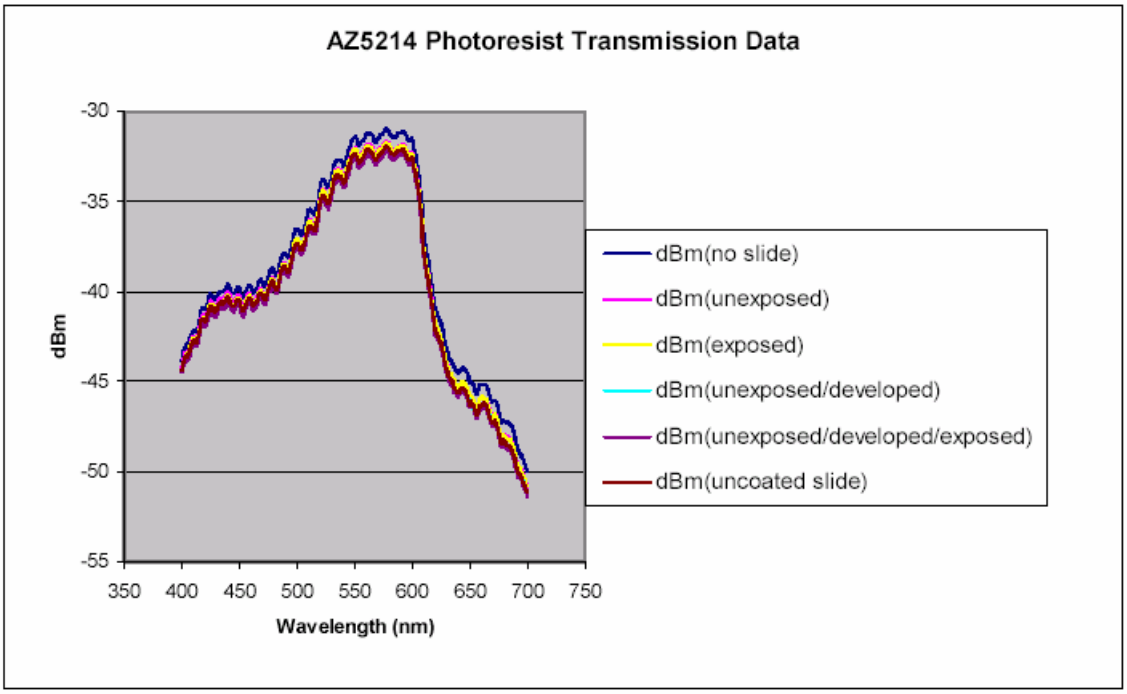

Figure 15: Spectral Transmission (400 nm to 700 nm)

It is important to note that even for the case of "no slide" in the set up, that the optical powers above 600 nm were low (less than –40 dBm). The literature from the manufacturer of the white light source claims that the optical power should be nearly equivalent through the entire visible spectrum. Thus, it is likely that there was a misalignment or operator error involved in the use of the spectrum analyzer. This will be investigated in more detail. Regardless, when the white light was blocked and prevented from entering the microscope objective, the output of the spectrum analyzer vanished. Similarly, when the fiber coming out of the white light source was directly inserted into the spectrum analyzer, the same overall profile was measured. Therefore, we thought that for purposes of this simple test it was appropriate to proceed.

In Figure 16, the percent difference in transmission is compared for the 5 cases against the transmission when no slide was placed in the set up.

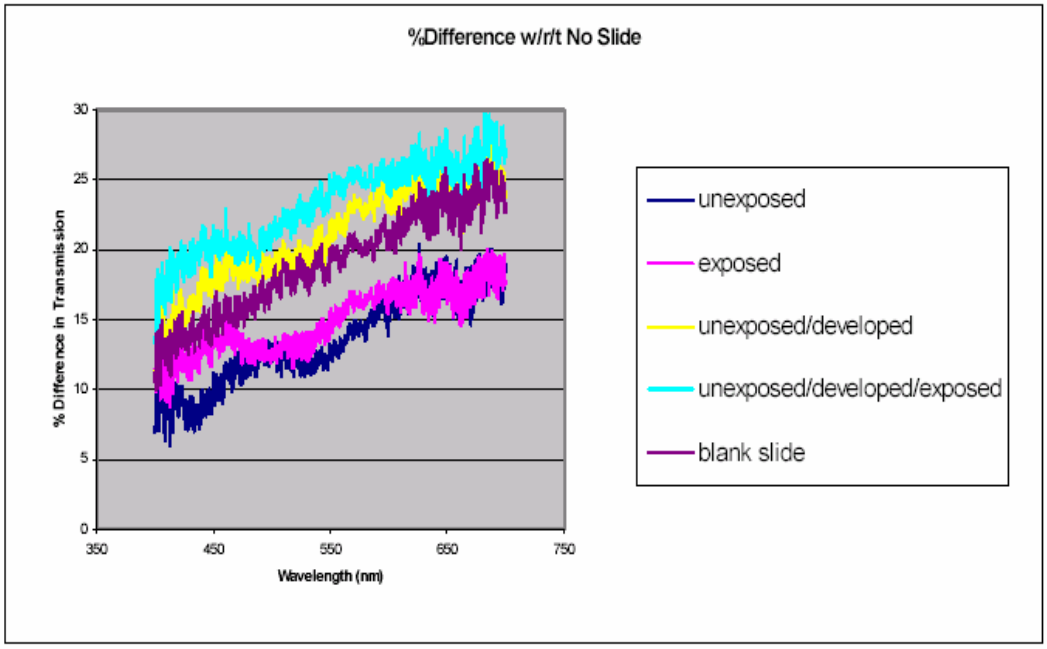

Figure 16: Percent Difference in Transmission

One would suspect that the blank slide would exhibit the lowest transmission loss. However, it falls in the middle. The increasing losses with wavelength are probably a result of the sharp decrease in overall optical power. This would tend to increase the margin of error in the measurement.

5.0 Conclusions

The OptoFlow project was aimed at modeling optical detection systems in micro-TAS, with a view to providing CAD tools that will enable the design of microfluidic microsystems containing integrated optical subsystems. The key to enabling this design is to provide tools that help designers with co-Design problems – that is, the ability to interface with several different microsystem domains that are typically present in these devices. The OptoFlow provides these results through releases of software at regularly scheduled intervals. We also expect to facilitate technology transfer through the released software and by creating a pathway for software enhancement based on the original plans as well as user feedback.